

A DETAILED LIST OF RESPONSES

TO REVIEWER #1

We greatly appreciate your careful reading of the manuscript, insightful comments, and valuable suggestions. Your thoughtful review has enhanced our paper considerably. The manuscript has been revised thoroughly according to your comments, with our point-by-point responses detailed below.

(1) Section 2.2: It is suggested to elaborate missing data handling, as it is one of the tricky part of the observational data while considering several meteorological parameters.

Response: Many thanks for your comments. The meteorological station data we used was from the China Meteorological Administration (CMA; <http://data.cma.cn/>), from 1961 to 2022. These data have missing values at different time periods, and we did not fill in the time series for the missing values, because any filling method will introduce errors.

To avoid potential human errors in filling in missing data in the time series, we exclusively perform spatial interpolation on the observational data, using only the available data.

Here, we provide an example using temperature data. Only stations available each day are used for interpolation, despite daily variation. In Fig. R1, red dots indicate stations with increased data compared to the previous decade, showing a growing number of stations available for spatial interpolation over time. In Section 2.2 (Lines 152-153) we added the following: “For missing values, we did not fill in the time series, but used only stations with available data for spatial interpolation each day.”

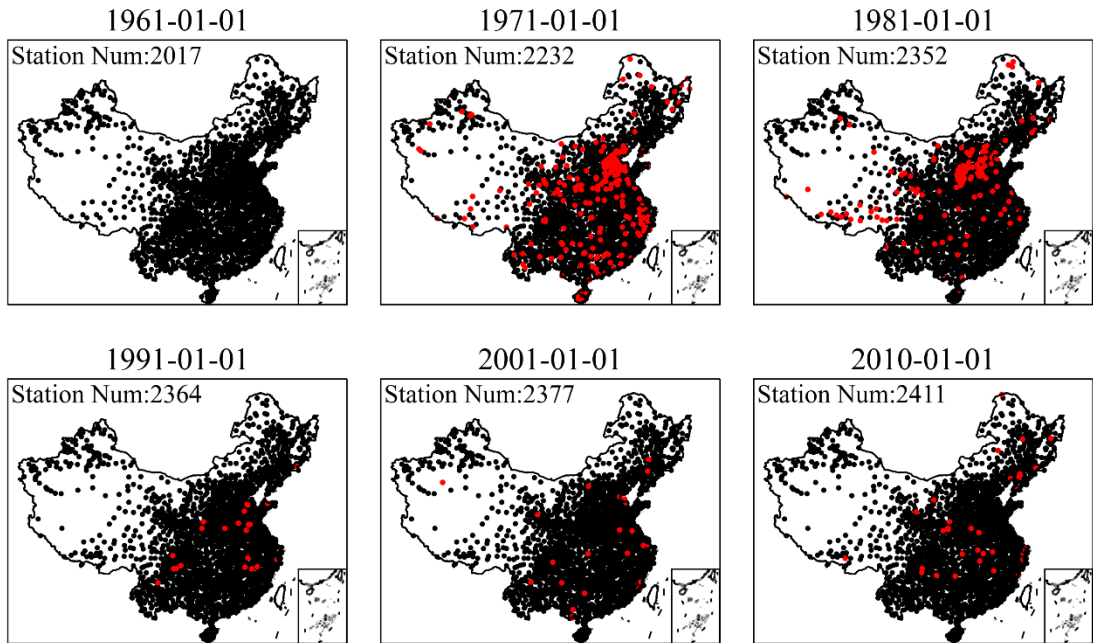


Fig. R1. Spatial distribution of average temperature (Tmean) monitoring stations over time. Black dots represent stations that existed in the previous time period, while red dots indicate stations newly added compared to the earlier time frame.

(2) Why angular distance-weighted interpolation (ADW) is considered for the higher-resolution gridding? Is it better than optimum interpolation method and state-of-the-art objective analysis techniques? Considering variability of meteorological parameters taken in this study, does ADW reasonable for all parameters?

Response: Many thanks for your comments. There are indeed many spatial interpolation methods. Our team's previous work has proved that the ADW method is the most suitable for precipitation interpolation (Han et al., 2023). The advantage of ADW is that it takes into account both the distance and angular relationships between stations, making it more robust in areas where data points are sparsely or irregularly distributed. This dual weighting system allows for more accurate interpolation in complex geographical settings, providing more reliable results for high-resolution gridding. Second, to maintain the consistency of the interpolation method, we apply the ADW method to all variables and consider the correlation decay distance (CDD) for each variable. ADW with CDD provides a key benefit that other methods may not

emphasize as directly: the gradual reduction of correlation with increasing distance between stations. By explicitly modeling the decay of correlation between station pairs (e.g., as illustrated for all variables in Fig. R2-R7), CDD ensures that distant stations contribute less to the interpolation, while nearby, highly correlated stations are given more weight. This distance-weighting characteristic is critical in regions with uneven station distributions, where ADW can mitigate the influence of distant stations that may not reflect local conditions accurately. In Section 2.2 (Lines 148-152) we added the following: “Before calculating the drought index, we interpolated the basic meteorological variables (Tmax, Tmin, Tmean, Wind, Ssd, Rh; see Figure 2) and considered the correlation decay distance (CDD) for each variable, and in the interpolation process we adopted angular distance-weighted interpolation (ADW), which considers angular weight in addition to the distance weight function, making it more robust to outliers. ADW with CDD provides a key benefit that other methods may not emphasize as directly: the gradual decrease of correlation with increasing distance between stations.”

Compared to the optimal interpolation (OI) method, ADW offers a simpler computational process suited for fast processing of large-scale data, making it ideal for real-time applications. ADW is particularly effective in regions with complex terrain, such as China, where it can handle spatial heterogeneity and provide smoother transitions across varying geographic and climatic conditions. Studies show that ADW more accurately captures spatial variations and reduces interpolation error in meteorological data. For instance, Chen et al. (2024) generated a high-accuracy raster dataset of China’s extreme temperature indices (1961–2020) using ADW, verifying its strong applicability in China.

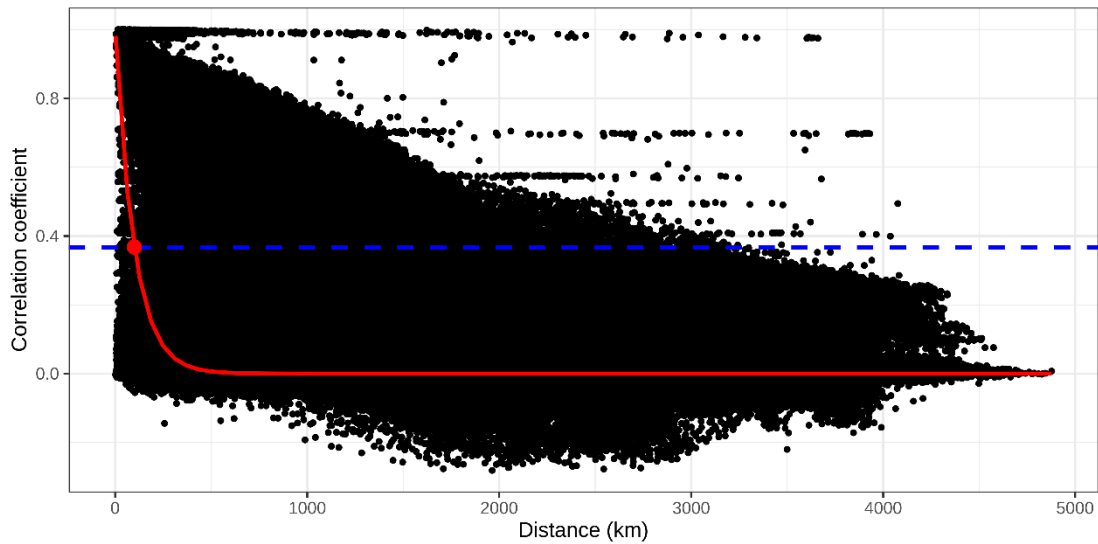


Fig. R2. Estimation of correlation decay distance (CDD ≈ 99) for daily mean temperature (Tmean) series for all stations in the interpolated domain. Black points show the distance–correlation pair for each station. The red line is the exponential curve fitted to the data by ordinary least squares. The blue dashed line marks where correlation equals $1/e$.

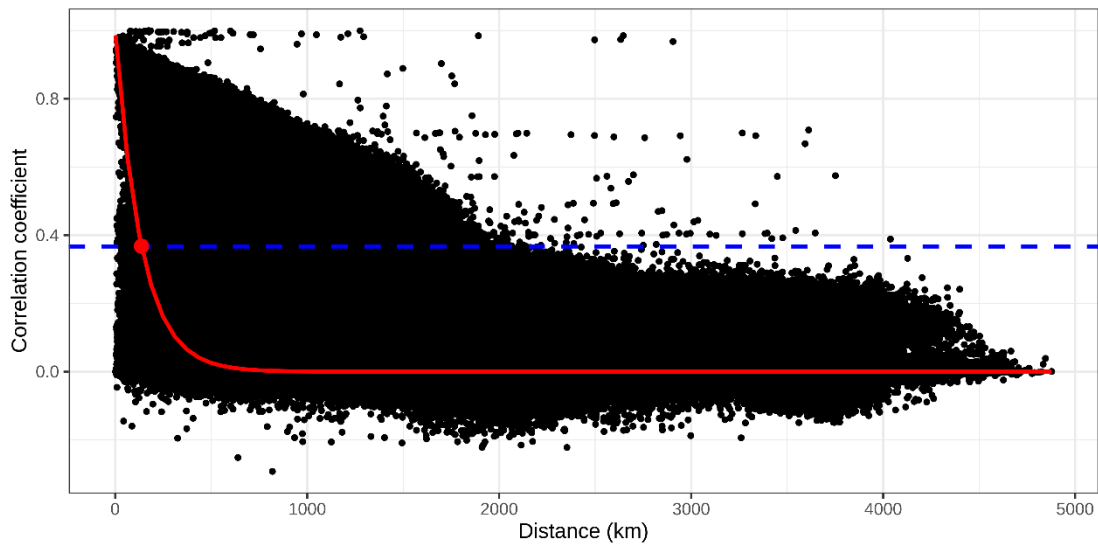


Fig. R3. Estimation of correlation decay distance (CDD ≈ 136) for daily min temperature (Tmin) series for all stations in the interpolated domain. Black points show the distance–correlation pair for each station. The red line is the exponential curve fitted to the data by ordinary least squares. The blue dashed line marks where correlation equals $1/e$.

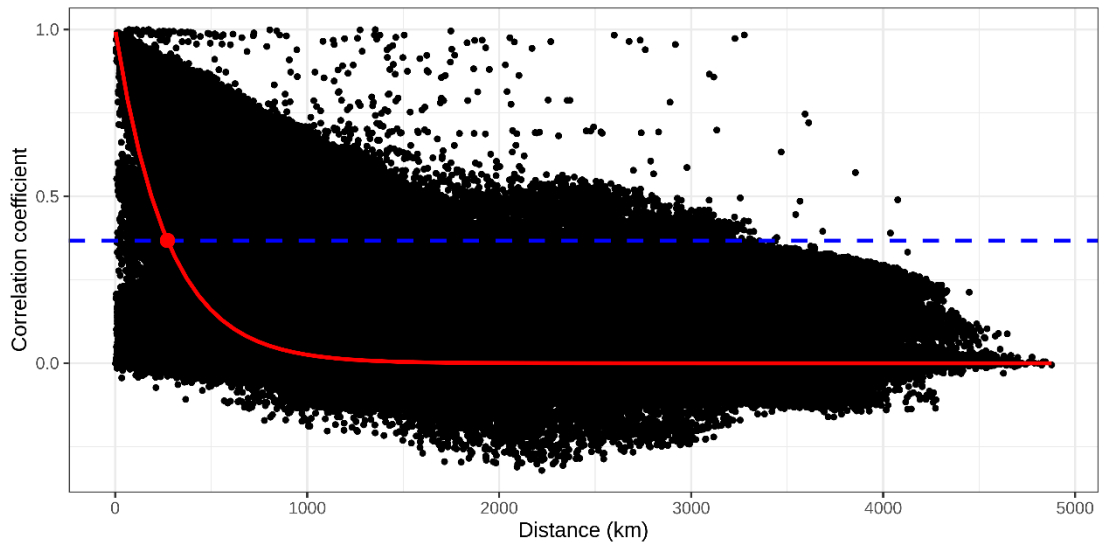


Fig. R4. Estimation of correlation decay distance (CDD ≈ 272) for daily max temperature (Tmax) series for all stations in the interpolated domain. Black points show the distance–correlation pair for each station. The red line is the exponential curve fitted to the data by ordinary least squares. The blue dashed line marks where correlation equals $1/e$.

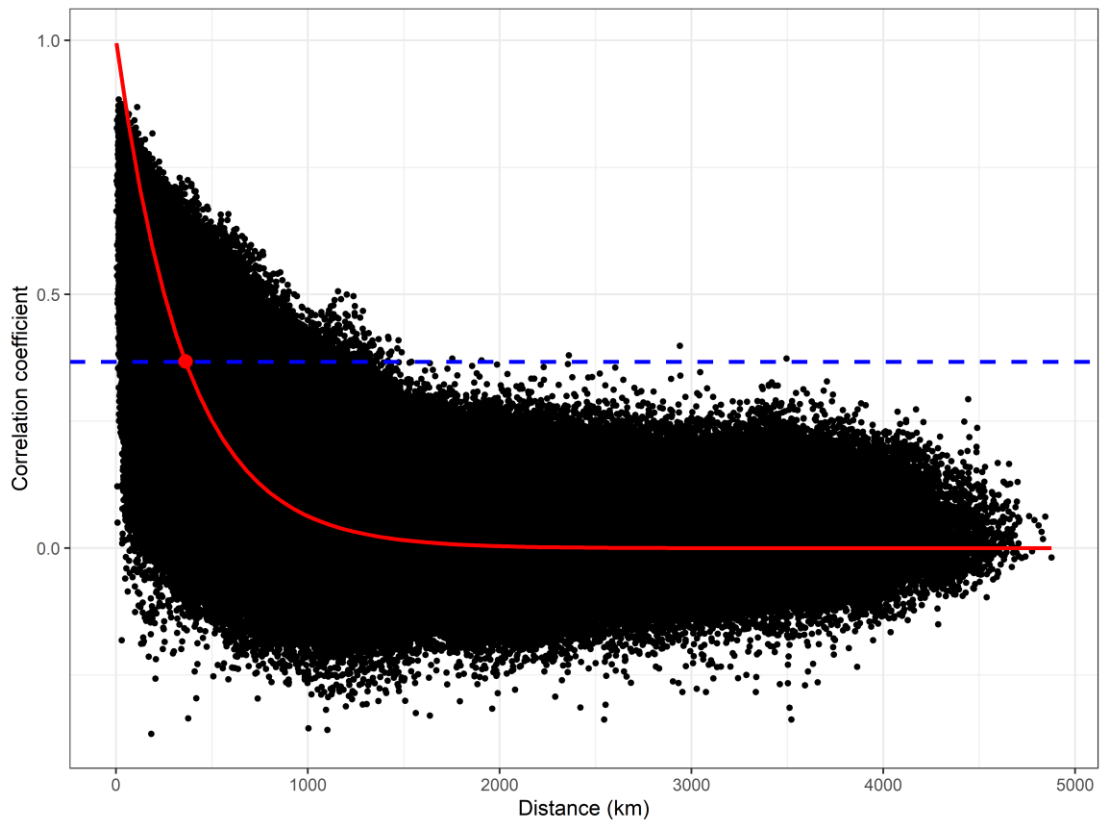


Fig. R5. Estimation of correlation decay distance (CDD \approx 361) for daily wind speed (Wind) series for all stations in the interpolated domain. Black points show the distance–correlation pair for each station. The red line is the exponential curve fitted to the data by ordinary least squares. The blue dashed line marks where correlation equals $1/e$.

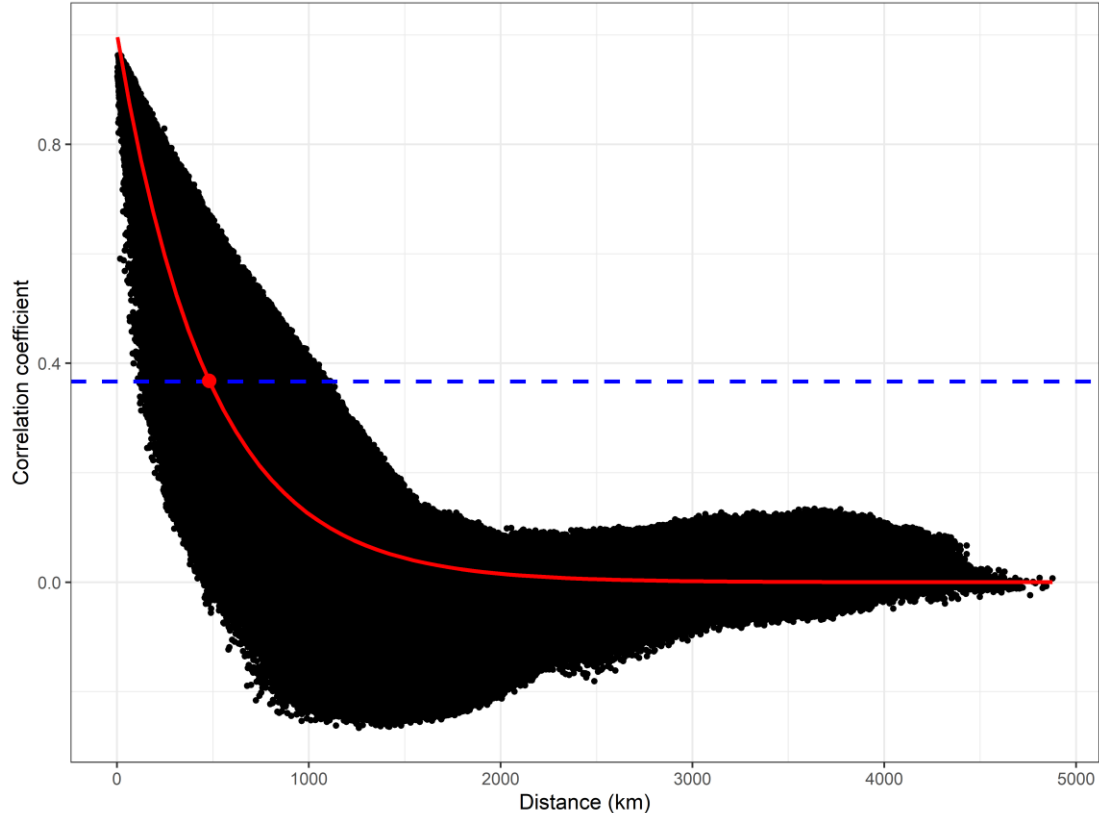


Fig. R6. Estimation of correlation decay distance (CDD \approx 480) for daily sunshine duration (Ssd) series for all stations in the interpolated domain. Black points show the distance–correlation pair for each station. The red line is the exponential curve fitted to the data by ordinary least squares. The blue dashed line marks where correlation equals $1/e$.

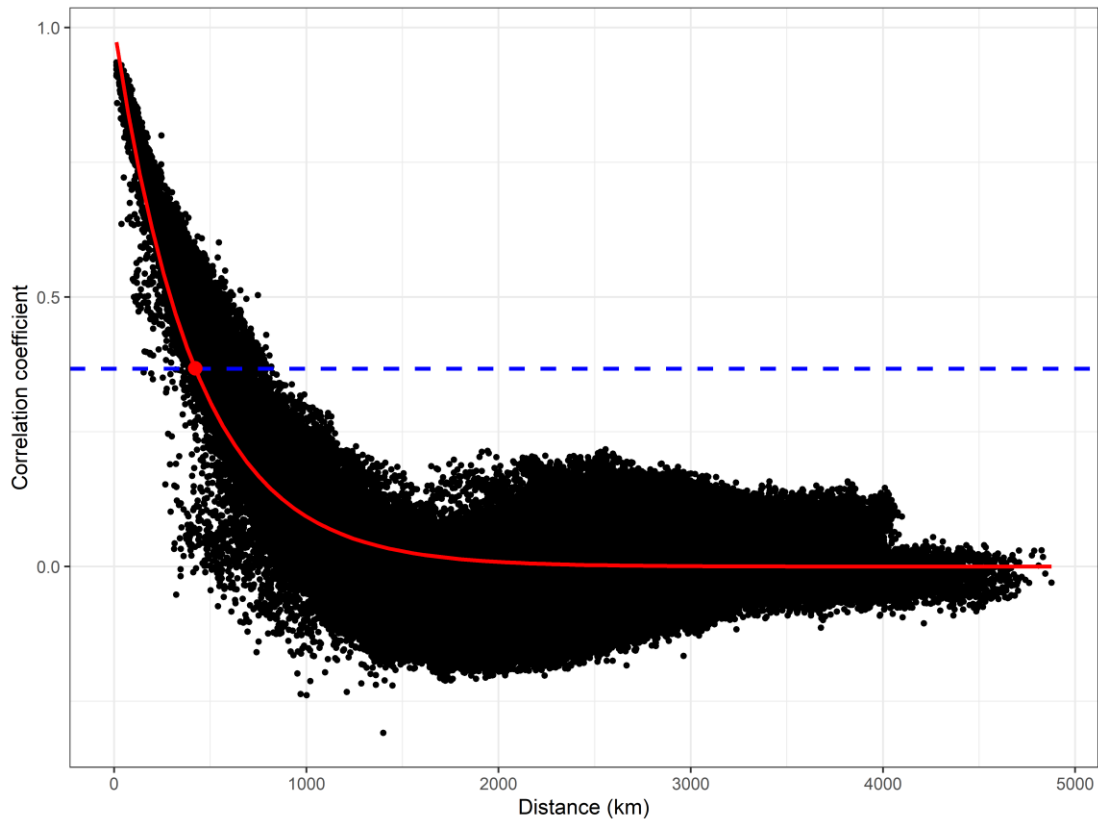


Fig. R7. Estimation of correlation decay distance (CDD ≈ 420) for daily average relative humidity (Rh) series for all stations in the interpolated domain. Black points show the distance–correlation pair for each station. The red line is the exponential curve fitted to the data by ordinary least squares. The blue dashed line marks where correlation equals $1/e$.

(3) Why authors have not considered multivariate drought indices including precipitation and soil moisture? An example of such long-term global datasets can be found at <https://doi.org/10.1088/1748-9326/7/4/044037>

Response: Many thanks for your comments. Considering that different drought indices can characterize different types of drought, and that there are so many drought indices to date, in this work we focus only on meteorological drought, which is a precursor to other types of drought. Accurate analysis of meteorological droughts is essential for predicting and understanding the development of other droughts, such as agricultural and hydrological droughts. By first conducting in-depth research on meteorological drought, we can lay the foundation for subsequent research on multiple drought types,

and improve the accuracy of overall drought monitoring and early warnings. Considering a multivariate drought index could indeed allow more comprehensive drought analysis; however, other data (such as soil moisture data) are difficult to obtain, and there are shortcomings in data quality and spatiotemporal coverage. Therefore, we plan to gradually introduce and integrate multiple-drought-type data in future studies to achieve more comprehensive drought assessment.

Additionally, as noted in the work of Aghakouchak and Nakhjiri (2012), the integration of GPCP and satellite data facilitates robust monitoring of past and near-real-time meteorological drought conditions through SPI calculation; however, their approach focuses solely on precipitation. Our study, on the other hand, calculates multiple indices that require a broader range of meteorological variables. For example, the calculation of potential evapotranspiration (PET), as used in the SPEI, requires variables such as precipitation, temperature, sunshine duration, and wind speed. Moreover, most satellite products lack key variables such as relative humidity and sunshine duration, which is why we rely on high-quality interpolated meteorological data for our drought index calculations.

(4) Yangtze River basin may be highlighted in any one figure for the convenience of the global readers.

Response: Many thanks for your comments. CHM_Drought covers the entire country from 1961 to 2022. For demonstration, in Section 4.1 of the paper, we take the summer of 2022 in the Yangtze River Basin as an example to examine the monitoring capabilities of each drought index. In the original, we used national data and did not show the scope of the Yangtze River basin, so we revised the manuscript to include the Yangtze River basin boundary to aid international readers. Among them, SPI, SPEI, and EDDI have multi-scale characteristics, so we show SPI, SPEI, and EDDI at a three-month scale (June, July, August; JJA) in Figure 3, while PDSI_China, SC-PDSI, and VPD represent mean summer (JJA) values. In addition, since the drought in the Yangtze River Basin this summer was prolonged, persisting into autumn, different time scales of the drought index could be used to monitor the initial hot spot of the drought and the

drought conditions caused after a long accumulation time. Similarly, the boundary of the Yangtze River Basin was also included in Figure 4. In Section 4.1 (Lines 285-287) we added the following: “A severe drought occurred in the south of China in the summer of 2022, mainly concentrated in the Yangtze River basin. To show the performance of the CHM Drought dataset in monitoring drought, we use the summer (June, July, August; JJA) of 2022 in the Yangtze River Basin as an example to examine the monitoring capabilities of drought indices.”

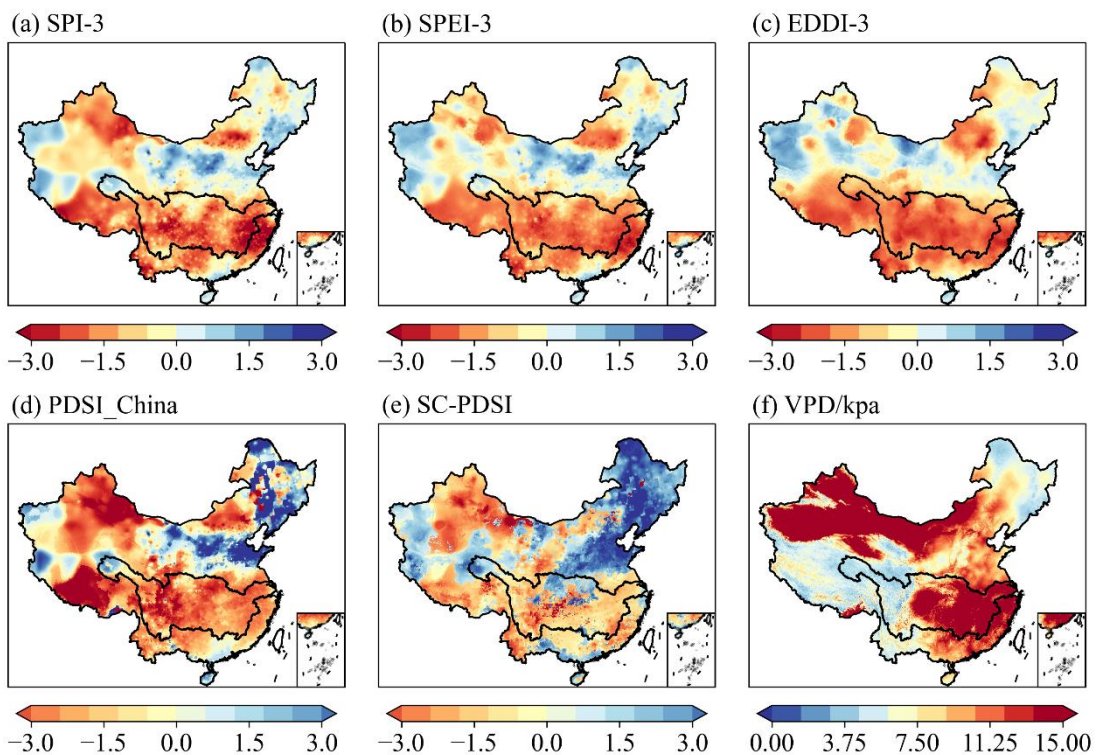


Figure 3: Spatial distribution of summer (June, July, August; JJA) drought characteristics in the Yangtze River Basin, China. Here, (a), (b), and (c) depict the three-month scale spatial distribution of drought indices, while (d), (e), and (f) present the average summer (JJA) values for these indices.

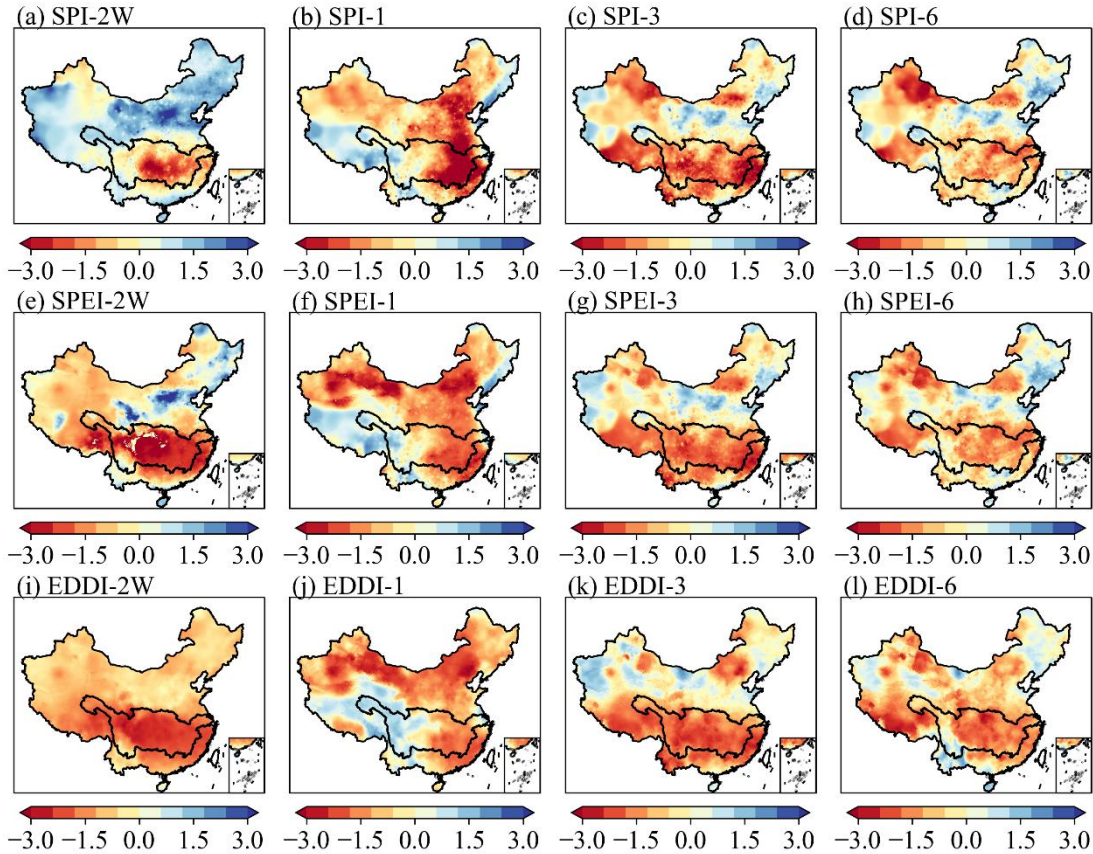


Figure 4: Spatial distribution of three drought indices (SPI, SPEI, and EDDI) in the Yangtze River Basin, China, across multiple timescales (2-week, 1-month, 3-month, and 6-month), using August 2022 as an example. (a–d) SPI-2W shows the 2-week scale SPI, SPI-1 shows the 1-month scale SPI, SPI-3 shows the 3-month scale SPI, and SPI-6 shows the 6-month scale SPI. The scales of SPEI and EDDI follow the same naming pattern.

(5) How empirical constant of expression 8 was determined. It needs to be elaborated.

Response: Many thanks for your comments. We used the modified calculation method for China-specific PDSI provided by the China National Standard for Meteorological Drought Classification (Standard No. GB/T 20481-2017; hereafter referred to as GB/T) (Zhong et al., 2019) for the calculation of PDSI_China, which includes the empirical constant in Expression 8.

Comparisons done for 9 stations in 7 states by Palmer. (1965) indicated different $\sum \bar{D}_t K'_i$ values, and the average value of $\sum \bar{D}_t K'_i$ for these 9 stations (i.e., 17.67) was

taken as the numerator and the $\sum \bar{D}_j K'_i$ for a given region was taken as the denominator. GB/T sets a in expression 8 to 16.84 instead of 17.67 according to the results of An et al. (1985). Specifically, An et al. (1985) selected the relevant data from 12 meteorological stations (Beijing, Qingdao, Xian, Xuzhou, Hohhot, Taiyuan, Hanzhong, Jiamusi, Shenyang, Hankou, Wuzhou, and Kunming) to revise the Palmer drought degree model in the process of revising the weight factors. For the detailed formula, please refer to the supplementary document.

$$K_i = \frac{a}{\sum_{j=1}^{12} \bar{D}_j K'_j} K'_i \quad (8)$$

(6) What is the role of land use/ land cover on drought indices? Is it possible to introduce any new index considering land use/land cover change?

Response: Many thanks for your comments. Although land use and land cover (LULC) significantly impacts drought, particularly in agricultural and hydrological contexts, our focus is on meteorological variables such as precipitation and temperature. On the other hand, because our high-resolution drought index is based on observational data, meteorological data already reflect land-atmosphere interactions, including LULC changes. Thus, the effect of LULC is inherent, although not explicitly isolated in this study.

Our current priority is to develop the CHM_Drought dataset, focused on high-resolution meteorological drought indices across mainland China from 1961 to 2022. Integrating LULC changes for a more comprehensive drought index is a valuable goal for future research.

(6) It is suggested to prepare an uncertainty map for each drought index. It would be vital for end users.

Response: Many thanks for your comments. We quantified the uncertainty of each index using standard deviation (Figure S4). Among the 6 drought indices involved in the study, the CRU data lacked relative humidity variables when calculating VPD index, which could not be calculated. Therefore, standard deviation was calculated for

all indices except the VPD index (Figure S4). In Section 4.2 (Lines 363-365) we added the following: “In addition, we quantified the uncertainties of SPI, SPEI and EDDI at different time scales (Figure S4). We used standard deviation to quantify the results, which were similar to those in Figures S1–S3. The results all showed that the highest uncertainties were mainly found in areas with few stations.”

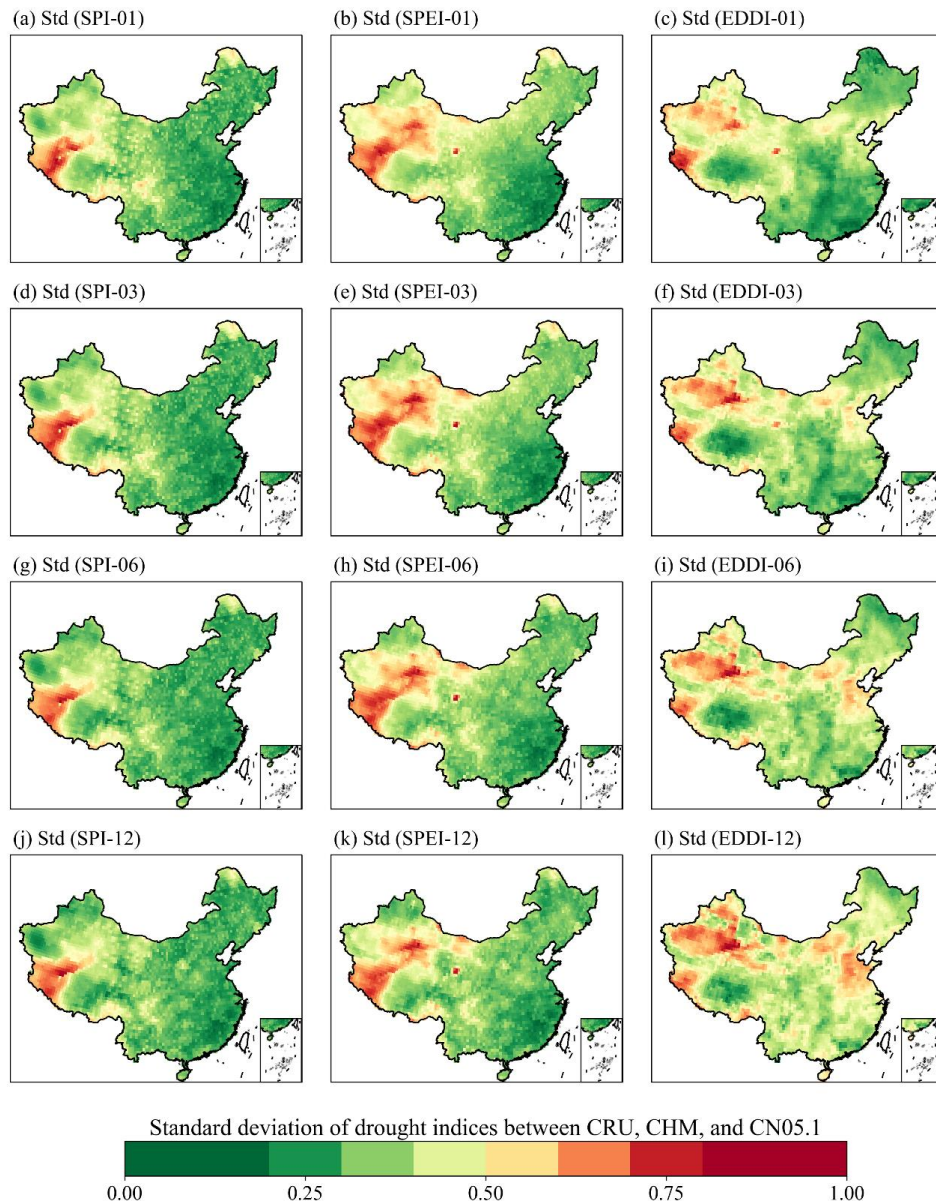


Figure S4: Spatial distribution of the standard deviations of the SPI, SPEI, and EDDI drought indices across three data sources (CRU, CHM, and CN05.1) at various time scales (1-, 3-, 6-, and 12-month). Here, (a-c) show the 1-month scale, (d-f) show the 3-month scale, (g-i) show the 6-month scale, and (j-l) show the 12-month scale.

References:

An, S., and Xing, J.: Modified Palmer drought index and its application, *Atmosphere*, 1985, (12):17-19 (in Chinese).

Aghakouchak, A. and Nakhjiri, N.: A near real-time satellite-based global drought climate data record, *Environmental Research Letters*, 7, <https://doi.org/10.1088/1748-9326/7/4/044037>, 2012.

Chen, Q., Zhang, Y., Liu, X., Lian, Q., and Xu, J.: Development of gridded dataset of extreme temperature index in China based on ETCCDI. *Journal of Global Change Data & Discovery*, 2024, 8(1): 67–75. <https://doi.org/10.3974/geodp.2024.01.08>.

Han, J., Miao, C., Gou, J., Zheng, H., Zhang, Q., and Guo, X.: A new daily gridded precipitation dataset for the Chinese mainland based on gauge observations, *Earth Syst Sci Data*, 15, <https://doi.org/10.5194/essd-15-3147-2023>, 2023.

Palmer, W. C., 1965: Meteorological drought. *Office of Climatology Research Paper 45*, Weather Bureau, Washington, D.C., 58 pp.

Zhong, R., Chen, X., Lai, C., Wang, Z., Lian, Y., Yu, H., and Wu, X.: Drought monitoring utility of satellite-based precipitation products across mainland China, *J Hydrol*, 568, <https://doi.org/10.1016/j.jhydrol.2018.10.072>, 2019.

----- end line -----
For your convenience, to make the review of our revisions easier, we have marked all responses and related revisions in light blue.